Available online at www.sciencedirect.com

SCIENCE DIRECT

PERGAMON

Polyhedron 22 (2003) 2045–2049

POLYHEDRON

www.elsevier.com/locate/poly

Structural and magnetic behavior of a quasi-1D antiferromagnetic chain compound $Cu(NCS)_2(pyz)$

H.N. Bordallo [a,b,*], L. Chapon [b,c], J.L. Manson [c,d], C.D. Ling [c,1], J.S. Qualls [e], D. Hall [f], D.N. Argyriou [b,c]

[a] *Intense Pulsed Neutron Source, Argonne National Laboratory, Argonne, IL 60439, USA*
[b] *Hahn-Meitner Institut, D-14109 Berlin, Germany*
[c] *Materials Science Division, Argonne National Laboratory, Argonne, IL 60439, USA*
[d] *Condensed Matter Sciences Division, Oak Ridge National Laboratory, Oak Ridge, TN 37831-6430, USA*
[e] *Department of Physics and Geology, University of Texas-Pan America, Edinberg, TX 78539, USA*
[f] *National High Magnetic Field Laboratory, Florida State University, Tallahassee, FL 32310, USA*

Received 6 October 2002; accepted 10 February 2003

Abstract

Synchrotron X-ray diffraction (XRD) and neutron powder diffraction (NPD) were used to determine the structure of $Cu(NCS)_2(pyz)$ (pyz = pyrazine = $C_4N_2H_4$), which consists of a stacking of Cu–pyz–Cu chains. While NPD measurements showed no evidence of long-range magnetic ordering, the temperature dependence of the magnetic susceptibility and magnetization suggests that the system can be adequately described on the *local* scale as a spin-1/2 antiferromagnet (AFM) chain with an intrachain exchange interaction $J/k_B = -8$ K (~ 0.7 meV). Comparison of isothermal magnetization data acquired up to 30 T at 1.6 K to a linear chain model shows excellent agreement, making this material a nearly ideal example of an isotropic Heisenberg AFM chain.

Keywords: X-ray diffraction; Neutron powder diffraction; Pyrazine; Quantum spin chain; Copper

1. Introduction

In recent years, it has been shown that exchange interactions mediated by organic ligands through long and complex pathways can lead to magnetic ordering at high temperatures [1]. As a result, much effort has focused on understanding the origin and role of such interactions [2]. Of the many diazine molecules that are known to bridge metal ions together, pyrazine (pyz) has been utilized extensively and shown to stabilize magnetic ordering temperatures up to 60 K [3–5]. Of the reported coordination polymers that contain pyz, most of them possess low-dimensional structures, i.e. 1D chains or 2D sheets. One notable exception is diamagnetic $Ag(pyz)_3(SbF_6)$ which has a 3D pseudo-cubic framework made up exclusively of Ag–pyz–Ag edges [6]. With this in mind, we sought to combine pyz and thiocyanate (NCS^-) anions in an attempt to form asymmetric lattices that may exhibit unusual magnetic properties. We have recently performed detailed structural and magnetic studies on $Fe(NCS)_2(pyz)_2$ which was determined to be a 2D Ising molecular magnet where 3D magnetic ordering is achieved [7]. While this system is a 3D antiferromagnet (AFM) below 6.6 K [8], its critical behavior is essentially 2D in nature. These findings suggested that in addition to the strong AFM coupling provided by pyz within the Fe–pyz–Fe sheets, the NCS^- anions that bound the Fe ions and stand above and below the Fe–pyz–Fe sheets (in an almost perpendicular fashion) must provide a weak interlayer exchange pathway. Indeed, the highly polarizable sulfur

---

* Corresponding author. Present address: Hahn-Meitner Institut, SF-1, Glienicker Strasse 100, D-14109 Berlin, Germany. Tel.: +49-30-8062-3174; fax: +49-30-8062-3094.

E-mail address: bordallo@hmi.de (H.N. Bordallo).

[1] Current address: Institut Laue-Langevin, F-38042 Grenoble Cedex 09, France.

0277-5387/03/$ - see front matter © 2003 Elsevier Science Ltd. All rights reserved.
doi:10.1016/S0277-5387(03)00188-8

atom may interact with the delocalized π-cloud of the nearly vertically oriented pyz ligands of neighboring squares.

By using the same molecular species, i.e. pyz and thiocyanate, we have created a new quasi-1D system, $Cu(NCS)_2(pyz)$, and herein we report its structure and magnetic properties. We find that although the NCS^- anions *also* bridge two Cu centers together, in contrast to $Fe(NCS)_2(pyz)_2$, this feature does not lead to long-range 3D ordering. Instead, we find that like copper pyrazine dinitrate, $Cu(pyz)(NO_3)_2$ [9], $Cu(NCS)_2(pyz)$ can also be described as an ideal 1D spin-1/2 Heisenberg AFM with nearest-neighbor interchange interaction $J \sim 0.7$ meV.

2. Experimental

A polycrystalline sample of $Cu(NCS)_2(pyz)$ was synthesized as follows: to a stirring 10 ml aqueous solution containing NH_4NCS (50.1 mmol, 3.813 g) and pyz (23.9 mmol, 1.914 g) was added a 10 ml aqueous solution of $Cu(NO_3)_2 \cdot 2.5H_2O$ (23.9 mmol, 5.559 g) to afford an olive green precipitate. The reaction mixture was stirred for ~ 2 h to ensure complete reaction and the solid collected via suction filtration. The sample was dried in vacuo for ~ 12 h yielding 5.28 g (85%) of $Cu(NCS)_2(pyz)$.

AC susceptibility measurements were carried out on a Lakeshore Model 7225 AC susceptometer between 1.6 and 16 K, with a 1-Oe drive field oscillating at 133 Hz. DC magnetization studies were carried out in a 1-kOe DC field, between 2 and 300 K, utilizing a Quantum Design MPMS-5S SQUID magnetometer. Isothermal magnetization measurements were carried out at 1.6 K at the National High Magnetic Field Laboratory in magnetic fields up to $\mu_0 H = 30$ T using an EG&G vibrating sample magnetometer. All measurements consisted of zero-field cooling to the lowest temperature and data collected upon warming.

Room-temperature synchrotron X-ray diffraction (XRD) data were collected on beam line 12BM-B (BESSRC-CAT) at the Advanced Photon Source. Data were acquired for $10° = 2\theta = 50°$ using a 2θ step-size of 0.005° and $\lambda = 1.0327$ Å. Time-of-flight neutron powder diffraction (NPD) was recorded on the Special Environment Powder Diffractometer (SEPD) at the Intense Pulsed Neutron Source (Argonne National Laboratory). Approximately 5 g of per deuterated $Cu(NCS)_2(pyz)$ was loaded into an aluminum sample can and mounted inside a standard closed-cycle He cryostat. Intensity data were collected at 300 K and between 4 and 25 K. All diffraction data were analyzed using the program GSAS [10].

3. Results and discussion

3.1. Crystal structure

In order to solve the crystal structure of $Cu(NCS)_2(pyz)$, we first obtained the size and type of the crystal system using the high-resolution XRD data. Here the location of observed reflections in 2θ were analyzed using the program TREOR developed by Visser [11] which assesses possible unit cells and space groups. Our analysis suggested a possible monoclinic crystal system which was subsequently confirmed by a fit of the powder pattern using the Le Bail method and the program GSAS [10] giving a monoclinic angle $\beta = 90.944(1)°$, and lattice constants $a = 10.7673(2)$ Å, $b = 6.96854(7)$ Å and $c = 5.6897(1)$ Å at 300 K (see Table 1). Upon successful indexing of both the X-ray and neutron powder patterns, a review of the observed reflections revealed systematic absences consistent with the monoclinic space group $C2/m$.

Owing to the low X-ray scattering factors (for all elements present except Cu), and the typically poor powder average of intensities due to the low X-ray penetration depth, the determination of the atomic positions and final refinement of the crystallographic structure of $Cu(NCS)_2(pyz)$ were performed using only NPD data. As the length of the b-axis is typical of Cu–Cu distances (6.46 Å) afforded when μ-bonded pyz exists (see, e.g. Ref. [9]), a starting model with Cu occupying the 2(a) (0, 0, 0) site was introduced in the calculation. F_0 nuclear density map, obtained from a Fourier inversion of observed intensities, was assembled and peak densities within it were identified at fractional coordinates (0, 0.254, 0) and (0.922, 0, 0.213), which correspond to the N atoms of the pyz ring and the thiocyanate ligand, i.e. N(1) and N(2), respectively. Incorporating these atoms into the calculation and performing successive cycles of Rietveld analysis and computation of difference ΔF Fourier maps permitted us to locate the remaining atoms in the structure. The final refinement ($R_p = 0.0139$, $R_{wp} = 0.03606$, $R(F^2) = 0.0687$ and $\chi^2 = 1.397$) is shown in Fig. 1.

The structure of $Cu(NCS)_2(pyz)$ consists of parallel chains of Cu^{2+} ions bridged by bidentate pyz ligands organized along the b-axis, as shown in Fig. 2. Thiocyanate anions lie in the ac-plane and bridge the Cu–pyz–Cu chains together to afford a 2D rectangular grid. The bond distance between the terminal sulfur atom and the Cu of the next chain (represented in the figure by a dashed line) is 3.011(7) Å. The sheets pack in a staggered fashion so that the Cu ion of one sheet lies above (and below) the centroid of adjacent 2D networks (Fig. 3). The coordination sphere of each Cu site is Jahn-Teller elongated to give typical 4 short+2 long bond geometry. The Cu chromophore is comprised of four nitrogen (from two pyz and two NCS^-) and two S

Table 1
Lattice parameters for $Cu(NCS)_2(pyz)$ at selected temperatures

T (K)	a (Å)	b (Å)	c (Å)	β (°)	Volume (Å^3)
4	10.5922(2)	6.9558(1)	5.6689(1)	91.915(2)	417.40(1)
50	10.6006(2)	6.9557(1)	5.6708(1)	91.877(1)	417.91(1)
100	10.6267(2)	6.9567(1)	5.6739(1)	91.718(1)	419.27(1)
150	10.6589 (2)	6.95891(9)	5.6777(1)	91.522(1)	420.99(1)
200	10.6946(2)	6.96203(9)	5.6815(1)	91.318(1)	422.92(1)
300	10.7673(2)	6.96854(7)	5.6897(1)	90.944(1)	426.86(1)

atoms. The Cu–N(1) and Cu–N(2) bond distances were found to be 2.088(2) and 1.914(2) Å, respectively. The sheets are separated by 5.38 Å, and consequently, very weak inter-sheet interactions are expected. Cohesion between the chains, within a sheet, is insured by the Cu–S bond that may further stabilize the 3D crystal structure. However, there is no evidence that it provides a super-exchange (SE) pathway. Indeed, no magnetic Bragg reflection was observed in the NPD data, indicating that $Cu(NCS)_2(pyz)$ does not show long-range magnetic ordering down to the lowest measured temperature (4 K).

3.2. Magnetic properties

Fig. 4 illustrates the temperature dependence of the DC magnetization ($\chi_{DC}(T)$) and the AC susceptibility $\chi'_{AC}(T)$, which shows a broad maximum at 7 K. This hump is generally associated with low-dimensional spin ordering. Indeed, a fit of $\chi_{DC}(T)$ to a 1D Bonner–Fisher uniform chain model [12] yielded $J/k_B = -7.67(4)$ K (~ 0.7 meV) and $g = 2.174(1)$. The obtained g-value is in good agreement with those reported for other Cu compounds [9,13,14]. Furthermore, electronic structure

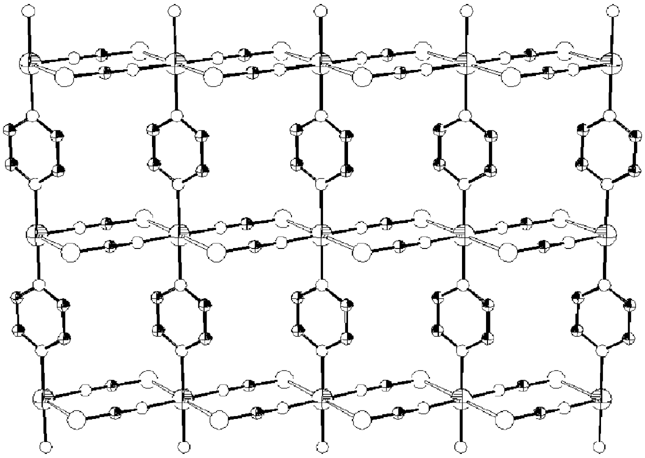

Fig. 2. 2D network structure of $Cu(NCS)_2(pyz)$ showing the cross-linking Cu–pyz–Cu and Cu–NCS–Cu chains. The Cu, S, N and C atoms are shown as octant-shaded, large open, small open and dark spheres, respectively. Deuterium atoms on the pyz ring have been omitted for clarity.

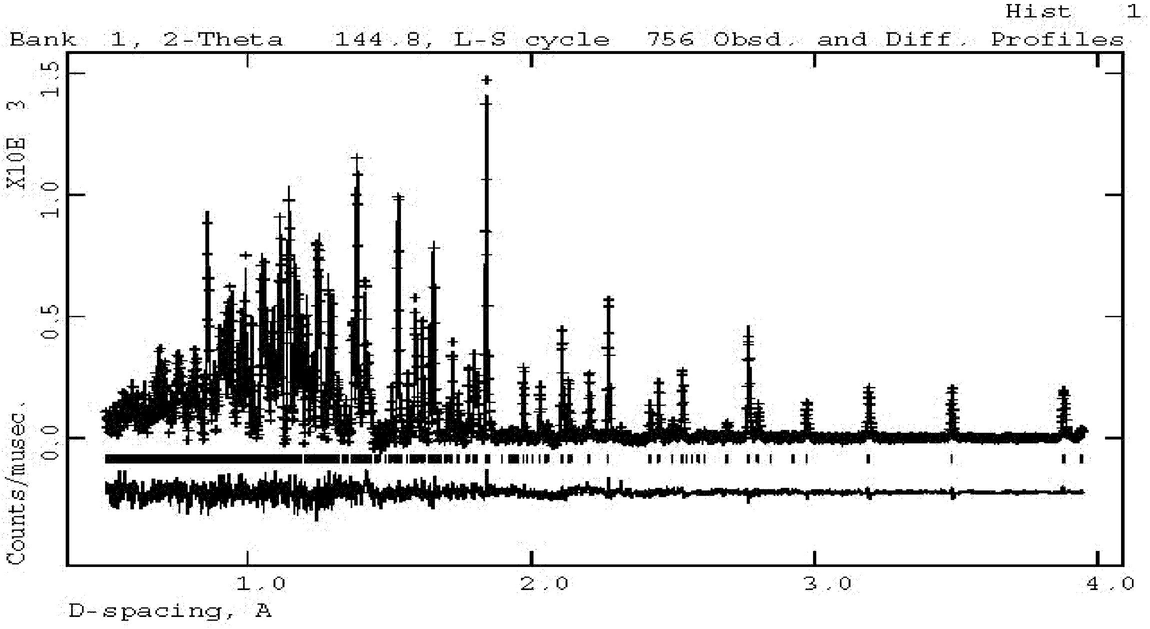

Fig. 1. Room-temperature neutron diffraction pattern obtained for $Cu(NCS)_2(pyz)$. The experimental data are shown as points and the Rietveld fit to the data is shown as a solid line, and the difference between experimental and calculated intensities is shown at the bottom.

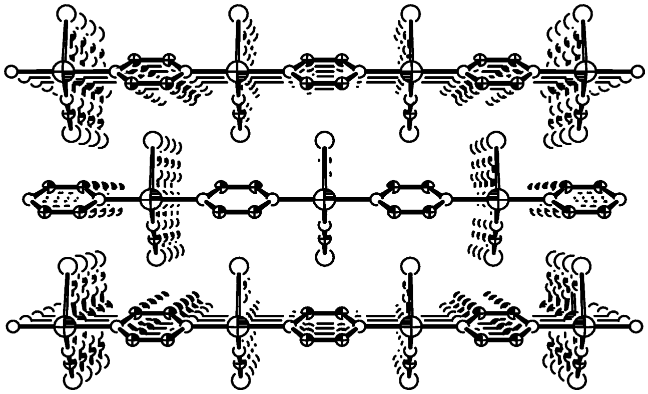

Fig. 3. Crystal packing of the 2D layers in Cu(NCS)$_2$(pyz). The Cu, S, N and C atoms are shown as octant-shaded, large open, small open and dark spheres, respectively. Deuterium atoms have been omitted for clarity.

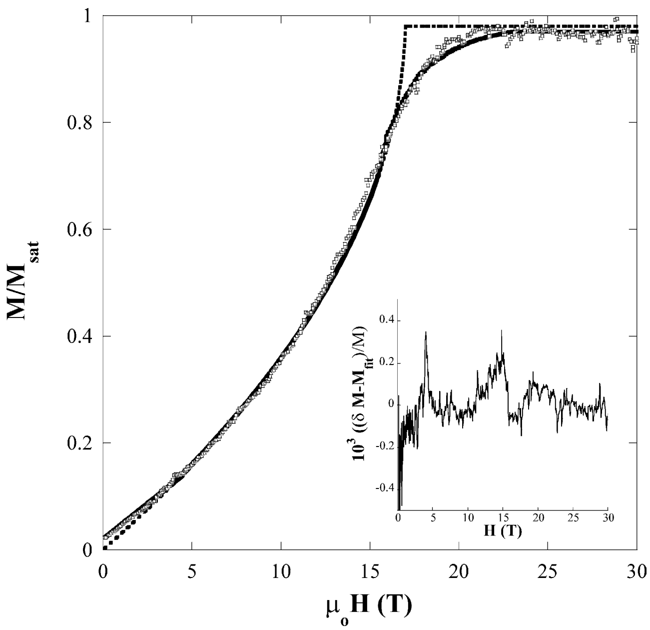

Fig. 5. Relative magnetization, M/M_{sat} (○) of Cu(NCS)$_2$(pyz) at 1.6 K. The dashed line is the calculated magnetization as a function of magnetic field for an $S=1/2$ AFM chain with $J/k_B = 8$ K at $T=0$ [16]. The continuous line is the result to a fit considering a finite chain model ($N=16$ spins 1/2) [13]. The residual ($\delta M - M_{fit}$)/M is shown in the inset.

calculations suggested that the super-exchange interaction is ~1500 times stronger along the Cu–pyz–Cu chain than between the chains through NCS$^-$ anions [3].

The relative magnetization, M/M_{sat}, obtained at 1.6 K for a polycrystalline sample of Cu(NCS)$_2$(pyz) as a function of field H up to 30 T is shown in Fig. 5. The observed behavior is very similar to other 1D spin-1/2 AFM chains [9,14,15]. Upon increasing field, the magnetization increases gradually and becomes nonlinear for fields larger than 4 T. Moreover, close to the saturation point, at $H \sim 18$ T, the positive concave feature reflects the AF ordering. As shown in the same figure, below 16 T the evolution of $M/M_{sat}(H)$ of Cu(NCS)$_2$(pyz) agrees quite well with the theoretical curve for a infinite linear spin-1/2 AFM chain with a Heisenberg exchange interaction and $J/k_B = -8.0(1)$ K at $T=0$ [16].

Now we turn to the comparison of the measured values of the magnetization to exact diagonalizations of linear chains containing up to $N=16$ spins 1/2 using the Bonner–Fisher Heisenberg model [13]. Using this model, we can accurately calculate the thermal and magnetic properties of quantum spin chains, and as a result determine if the short-range order can be theore-

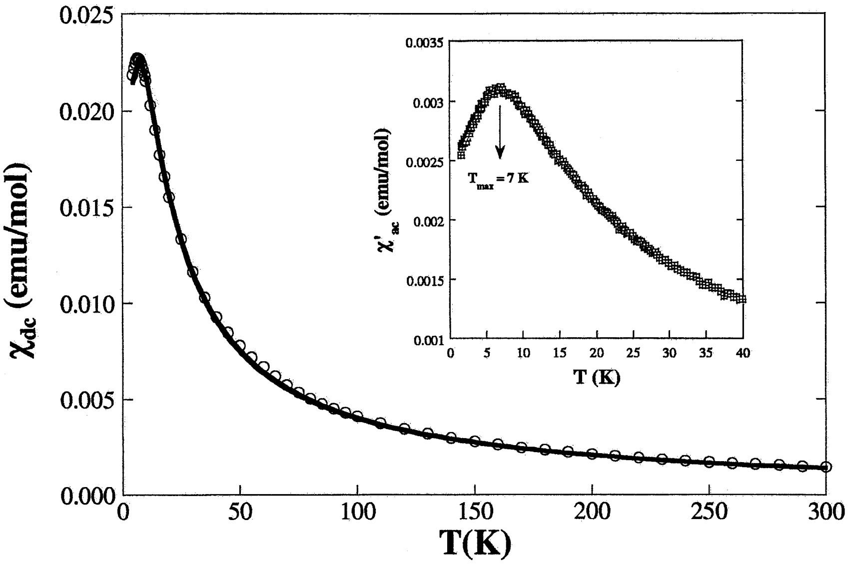

Fig. 4. $\chi_{DC}(T)$ (○) and theoretical fit (—) to the Bonner–Fisher 1D AFM chain as described in the text. The inset depicts $\chi'_{AC}(T)$ that shows a broad maximum indicative of short-range magnetic ordering.

tically explained by the 1D magnetic interactions. As shown in Fig. 5, the model is in excellent agreement with the experimental results, giving $J/k_B = -8$ K. Indeed, the Bonner–Fisher analysis of the magnetization data can only be distinguished from the experimental data near the saturation value. The residual of the fit is shown in the inset of Fig. 5. In conclusion, down to 1.6 K $Cu(NCS)_2(pyz)$ can be satisfactorily described by the linear chain model.

4. Conclusion

Pyrazine (pyz) is a classical bridging ligand that has been extensively used in the design of novel network structures and shown to stabilize magnetic ordering in molecule-based systems. Among them, we can cite $Mn[N(CN)_2]_2(pyz)$ and $Fe(NCS)_2(pyz)_2$, which have been characterized as 1- and 2D coordination polymers that display 3D magnetic ordering below $T_N = 2.53$ and 6.6 K, respectively [3,7,8]. In these compounds, the 3D ordering is mainly driven by the strength of the in-chain coupling, which determines the rate of increase of the spin correlation lengths within the M–pyz–M component. For the sake of comparison, we synthesized and characterized the 1D analog $Cu(NCS)_2(pyz)$.

By combining powder neutron and synchrotron XRD, the nuclear structure of $Cu(NCS)_2(pyz)$ was determined by successive Fourier analysis. As no new magnetic Bragg peaks are observed in the neutron data down to 4 K, we can conclude that 3D magnetic ordering does not occur in $Cu(NCS)_2(pyz)$. As a consequence, the broad feature observed on the magnetic susceptibility around 7 K probably indicates that magnetic ordering occurs only within the Cu–pyz–Cu chains. Furthermore, we showed that $Cu(NCS)_2(pyz)$ is extremely well described by the simple Heisenberg model of the $S = 1/2$ AFM spin chain with $J/k_B = -8.0(1)$ K (~ 0.7 meV). In light of what is known about $Cu(NO_3)_2(pyz)$, our results reveal that $Cu(NCS)_2(pyz)$ is an excellent candidate for further studies regarding quantum critical phenomena in spin-1/2 Heisenberg AFM.

5. Supplementary material

Crystallographic data for the structural analysis have been deposited with the Cambridge Crystallographic Data Center (CCDC No. 194926). Copies of this information may be obtained free of charge from The Director, CCDC, 12 Union Road, Cambridge, CB2 1EZ, UK (fax: +44-1223-336033; e-mail: deposit@ccdc.cam.ac.uk or www: http://www.ccdc.cam.ac.uk).

Acknowledgements

This work was benefited from the use of IPNS at ANL, funded by the US DOE Contract No. W-31-109-Eng-38. Work at Oak Ridge National Laboratory was supported by the US DOE under Contract No. DE-AC05-00OR22725 with UT-Battelle, LLC. Part of this work was performed at the National High Magnetic Field Laboratory, which is supported by NSF cooperative agreement No. DMR-9527035 and the State of Florida.

References

[1] M. Verdaguer, A. Bleuzen, C. Train, R. Garde, F. Fabrizi de Biani, C. Desplanches, Phil. Trans. R. Soc. London Ser. A 357 (1999) 2959.

[2] A.J. Epstein, MRS Bull. 25 (2000) 33.

[3] J.L. Manson, Q.-Z. Huang, J.W. Lynn, H.J. Koo, M.H. Whangbo, R. Bateman, T. Otsuka, N. Wada, D.N. Argyriou, J.S. Miller, J. Am. Chem. Soc. 123 (2001) 162.

[4] B.-Q. Ma, H.-L. Sun, S. Gao, G. Su, Chem. Matter 13 (2001) 1946.

[5] F. Lloret, M. Julve, J. Cano, G. De Munno, Mol. Cryst. Liquid Cryst. 334 (1999) 569.

[6] L. Carlucci, G. Ciani, D.M. Prosperpio, A. Sironi, Angewandte Chemie Int. Ed. English 34 (1995) 1895.

[7] L. Chapon, J.L. Manson, H.N. Bordallo, E.A. Goremychkin, D. Ravot, W. Reiff, J. Hernandez-Velasco, D.N. Argyriou, PRB, submitted for publication.

[8] J.A. Real, G.D. Minno, M.C. Munoz, M. Julve, Inorg. Chem. 30 (1991) 2701.

[9] P.R. Hammar, M.B. Stone, D.H. Reich, C. Broholm, P.J. Gibson, M.M. Turnbull, C.P. Landee, M. Oshikawa, Phys. Rev. B 59 (1999) 1008.

[10] L.C. Larson, R.B.V. Dreele, version 2002, 2002.

[11] J.W. Visser, J. Appl. Crystallogr. 2 (1969) 89.

[12] J.C. Bonner, M.E. Fisher, Phys. Rev. A 135 (1964) A640.

[13] P. Zhou, G.F. Tuthill, J.E. Drumheller, Phys. Rev. B 45 (1999) 2541.

[14] M. Azuma, T. Odaka, M. Takano, D.A. Vander Griend, K.R. Poeppelmeier, Y. Narumi, K. Kindo, Y. Mizuno, S. Maekawa, Phys. Rev. B 62 (2000) R3588.

[15] H. Mollymoto, E. Fujiwara, M. Motokawa, M. Date, J. Phys. Soc. Jpn. 48 (1980) 1771.

[16] R.B. Griffins, Phys. Rev. A 133 (1964) A768.